MICROSTRUCTURE - FAILURE MODE CORRELATIONS IN BRAIDED COMPOSITES

G. J. Filatovs and R. L. Sadler
North Carolina A&T State University, Greensboro, NC
A. El-Shiekh
North Carolina State University, Raleigh, NC

ABSTRACT

Explication of the fracture processes of braided composites is needed for modeling their behavior. Described is a systematic exploration of the relationship between microstructure, loading mode, and micro-failure mechanisms in carbon/epoxy braided composites. The study involved compression, and fracture toughness tests and optical and scanning electron fractography, including dynamic in-situ testing. Principal failure mechanisms of tow sliding, buckling, and unstable crack growth are correlated to microstructural parameters and loading modes; these are used for defining those microstructural conditions which are strength limiting.

INTRODUCTION

The integrated nature of multidimensional braided composites holds promise for overcoming some of the shortcomings of conventional laminate composites, while introducing compromises of their own. While their general behavioral trends are known there are still many knowledge gaps and obstacles to their use. In particular, the high anisotropy and interaction of several structural levels have made selection of representative volume elements and homogenization procedures difficult. At the present, no superior method of modeling and analyzing these materials has emerged.

This paper gives an overview of several projects focused on the deformation and failure of braided materials. The approach is experimental micromechanics-based, relying on testing of small-scale specimens and optical and SEM fractography. There is a prohibitively large number of material and braid geometry combinations to be exhaustively tested; therefore the focus has been on determining the failure sequence and failure controlling microstructural features. The goal is the establishment of a heuristic, rule-based description of the

failure process/microstructural interaction, and of the definition of a mechanical properties unit cell which can be used as a bridge to macro-scale behavior.

MATERIALS AND PROCESSES

The textile preforms were braided with 12K tows of Celion G30-500 (BASF Structural Materials, Inc.) graphite fibers. These fibers measure 7 microns in diameter and have a modulus of 30 Msi. The preforms were braided by a 4-step process in a 3 X 14 design where each of the tows is interlocked with the other tows to form a true 3-D structure. Reference [1] contains a discussion of the 4-step braiding process.

Composites are fabricated from these textile preforms using a vacuum/compression consolidation process. The matrix is comprised of two components, Epon 828 (Shell Chemical Company) and Jeffamine T-403 (Texaco Chemical Company), in a ratio of 100:42 parts-by-weight respectively. After mixing, the catalyzed resin is vacuum degassed for 10 minutes at < 1 Torr. The preform is placed in a mold and submerged in the liquid resin and the evacuation step is repeated. The mold is closed and the composite is press cured for 3 hours at 100 C. A mechanical stop is used to control the thickness of the composite. Typical dimensions for the composite samples are 0.100 X 0.750 X 10.0 inches. More details of the fabrication aspects are given in [2]. The fiber volume fraction was typically 55%.

Composite tubes were also used in these experiments. They were fabricated from a textile preform braided in much the same manner as the flat braid but the machine bed was circular instead of rectangular. The tube preforms were impregnated and consolidated by resin transfer molding (RTM) with Tactic 123 (Dow Chemical Co.) and catalyzed with Millamine 5260 (Milliken Chemical Co.) in a ratio of 100:17 parts-by-weight respectively. This matrix system requires a cure of 1 hour at 70^{o}C followed by 2 hours at 170^{o}C.

STRUCTURAL DESCRIPTION

A structural description of the composite is necessary for any consideration of failure modes. The preform structure has been defined from a textile point of view [1]. Such a description, however, is only partly descriptive of the final component. While computational unit cells have been proposed for braids and weaves [3,4], care must be taken in

extracting them from the actual structure. A different approach will be taken here.

Figures 1a and 1b show the textile preform and the subsequent composite coupon fabricated from it. In this case, a white tracer tow has been added indicating the location of a single tow. Figures 2a and 2b show the top and side views of a single tow extracted from the composite. Based on these, a schematic of the tow location, along with identification of the important microstructural descriptors and the surface/volume mapping can be constructed (Figure 3).

Note that a fiber tow lies on a diagonal-type plane and sinuously spans the thickness of the specimen. This fiber does not exactly match the apparent surface pattern. The true cycle length, or the return of the tow to its starting position may be quite long and depends on the braiding cycle. For the purpose here, it is sufficient to define one cycle as the return to the equivalent point on the diagonal plane. Figure 4 is a further idealization and contains only two representative crossing tows. The diagonal length of this cell is one half the cycle length previously defined.

Figure 4 can be used for creating an efficient representation of the tow structure. Consider a unit cell as commonly defined in x-ray crystallography [5]. This type of unit cell allows the use of Miller Indice notation, which describes directions, planar orientations, and directional relationships in compact form. The X, Y, and Z axes become [100], [010], and [001] respectively. The diagonal plane on which the tows lie are of the form (110), and the crossing points or intersection of the tows are generally on the (111)-type planes. The cell here is, of the the orthorhombic type, and actual cell parameters are established by measurement from the fabricated composite.

TEST RESULTS

Table 1 contains selected test results from small coupons, along with the external load conditions and specimen details. The matrix (neat resin) specimen failed along the expected 45^{o} shear lines. The axial specimens initially failed in shear along the apparent braid angle. SEM fractographs are shown in Figure 5. Internally, the failure was of a mixed mode on the (110) and (111)-type planes. Note the rapid drop in axial strength with the increase of braid angle. The overall trend with fiber volume fraction is shown in Figure 6. In later stages of the failure sequence fiber buckling occurred. For transverse compressive loading, the failure was tows sliding over each other on the (111)-type planes.

The notched specimens were based on ASTM E399 compact fracture toughness specimens [6]. This test was developed for metals but attempts have been made to use it for laminate composites. For braided materials this test appears useful only as a worst-case indicator. If the notch is along the braid direction, the specimen tends to fail in cleavage at values below that of the matrix. The crack front moves in general along the (110)-type planes. For notches perpendicular to the braid direction the failure load is considerably higher but the crack length, area and failure mode are difficult to determine. Figure 6 is an SEM of this case. Considerable additional work is required to remove uncertainties from the testing results.

Tests were also conducted on components. Axial compression of one inch diameter braided tubes and T-sections followed the same trends as the coupons. Figures 7 and 8 are micrographs of these specimens.

The loads and stresses given in Table 1 are those for yielding. There is much post-yield phenomena in these materials, with higher values possible with continued testing, along with increasing damage. At some point the damage becomes catastrophic and the specimen fails.

DISCUSSION

The previous results represent only selective, illustrative data. Our experience with these materials runs to hundreds of samples and a variety of tests, and these will be amplified in other publications. The common trends and generalizations that have emerged will be outlined here.

The dominant descriptive parameter is the braid angle. The differentiation between the apparent and internal braid angles is approximately 3^{o} for most braids, and the surface angle can be used as an approximation in most cases.

In the initial stages of the failure sequence, the tows act as units, giant pseudo-fibers. It is useful to partition the matrix into inter- and intra- tow components. The inter-tow matrix and fibers form the tows which are surrounded by the intra-tow matrix. If the total fiber fraction is V_{total}, and the fiber fraction in the tow is V_{tow}, then the inter-tow matrix fraction is

$$1 - V_{total} / V_{tow} \qquad (1)$$

This assumes the tows are straight.

Most tows are not circular; combined with tow curvature this has the effect that in later stages of failure the individual fibers in a tow do not carry the load evenly and failure occurs by sequential tearing. This is a strength lowering but energy absorbing mechanism.

Fiber-matrix interface debonding is frequently the initiating event in failure, allowing either tow sliding or the formation of cracks at resin-rich areas. It appears that the accumulation and growth of these cracks is encouraged by the resin-rich areas.

There is also a stochastic aspect introduced by structural variability. Most braided materials contain variation in the braiding angle, and this is linked in a complicated way to the local density and fiber volume. The variation in even high quality braids can be as much as 2 degrees. Considering the effect of braid angle on compressive strength given previously, there is bound to be an uncertainty in strength values of components. Further, in components, cracks in tension have a probability of being in the proper orientation for runaway crack growth.

Do these observations point the way to any solutions of the shortcomings? Stronger interfaces are one possibility. To reduce the effects of matrix-rich areas fewer fibers per tow or stress dispersants such as microballoons could be used. But the toughness/energy absorption vs. strength tradeoffs are not fully known, and much work remains in understanding these materials.

As a closure, the question of a mechanical properties unit cell will be considered. Based on the foregoing experimental work, it appears that this could be derived from the unit cell defined previously. This unit cell would reflect the fracture-strength anisotropy, and would contain scaled equivalent volumes of matrix and fiber. These would be corrected to reflect Equation 1, and the interface angles would be based on observed failure processes. Variability can be introduced by considering a distribution of cells. We have used such an approach by assigning failure criteria and using Weibull statistics, and have been able to model some macro failure processes. This work is continuing.

ACKNOWLEDGMENT

The work reported in this paper was supported in part by NASA grant No. NAGW-1331 to the Mars Mission Research Center, and by ONR Research Grant No. NOOO14-K-0682 to the Center for Composite Materials Research, both at N.C. A&T State University, Greensboro, NC.

REFERENCES

1. Wei Li and Aly El-Shiekh, "The Effect Of Processes And Processing Parameters On 3-D Braided Preforms For Composites", SAMPE Quarterly, Vol.19, No. 4, 1988, pp 22-28.

2. Bagher Bagherpour, "Microstructural Aspects Of Failure Modes Of Braided Composite Materials", MS Thesis, N.C. A&T State University, 1991.

3. J. Yang, C. Ma, and T. Chou,"Fiber Inclination Model Of Three-Dimensional Textile Structural Composites", J. Comp. Matl., Vol. 20, 1986, pp 472-483.

4. T. J. Whitney and T-W Chou, "Modeling Of 3-D Angle-Interlock Textile Structural Composites", J. Comp. Matl., Vol. 23, 1989, pp 890-911.

5. B. D. Cullity, "Elements Of X-Ray Diffraction", Addison-Wesley, 1956.

6. ASTM Standards, Section E399-79a.

Table 1 Test Results

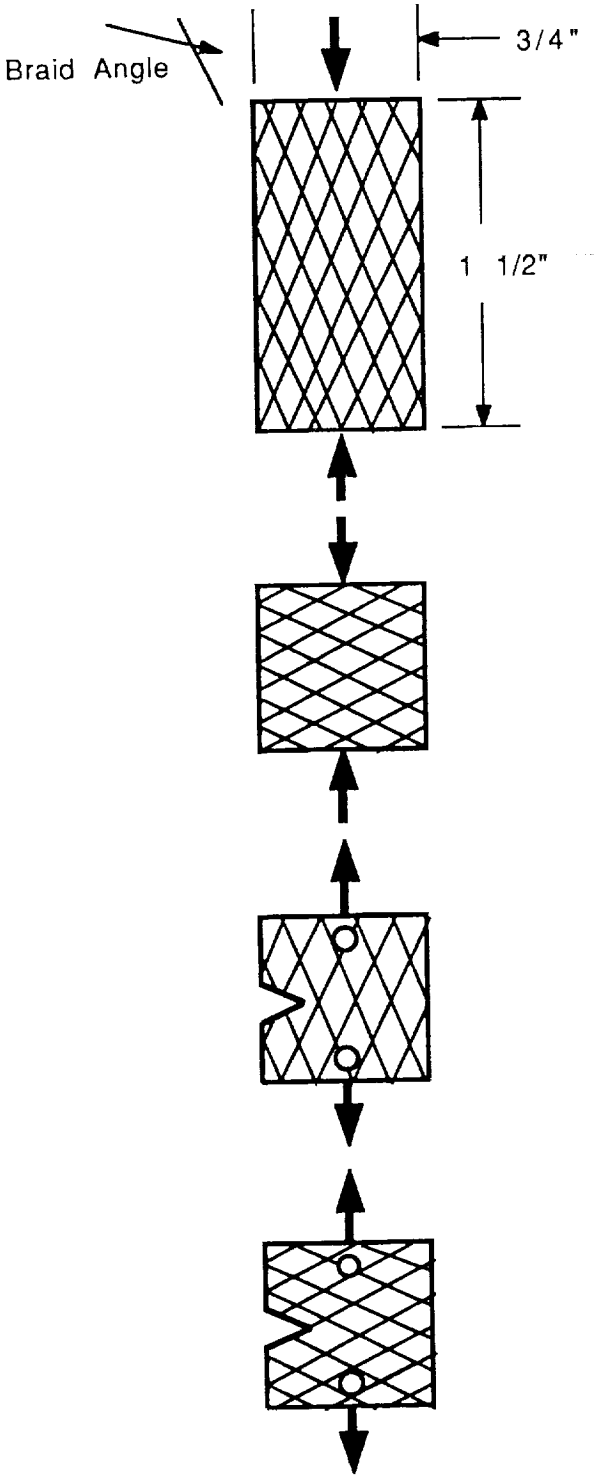

Angle	Axial Yield Stress
3	110,000 psi
13	66,000
18	44,000
23	16,000
Matrix	13,000

Fiber Volume - 55% approx.
Thickness - 0.100 approx.

Angle	Transverse Stress
21	5,000 psi

Angle	Notched Strength
21	140 pounds

Angle	Notched Strength
21	52 pounds
Matrix	60 pounds

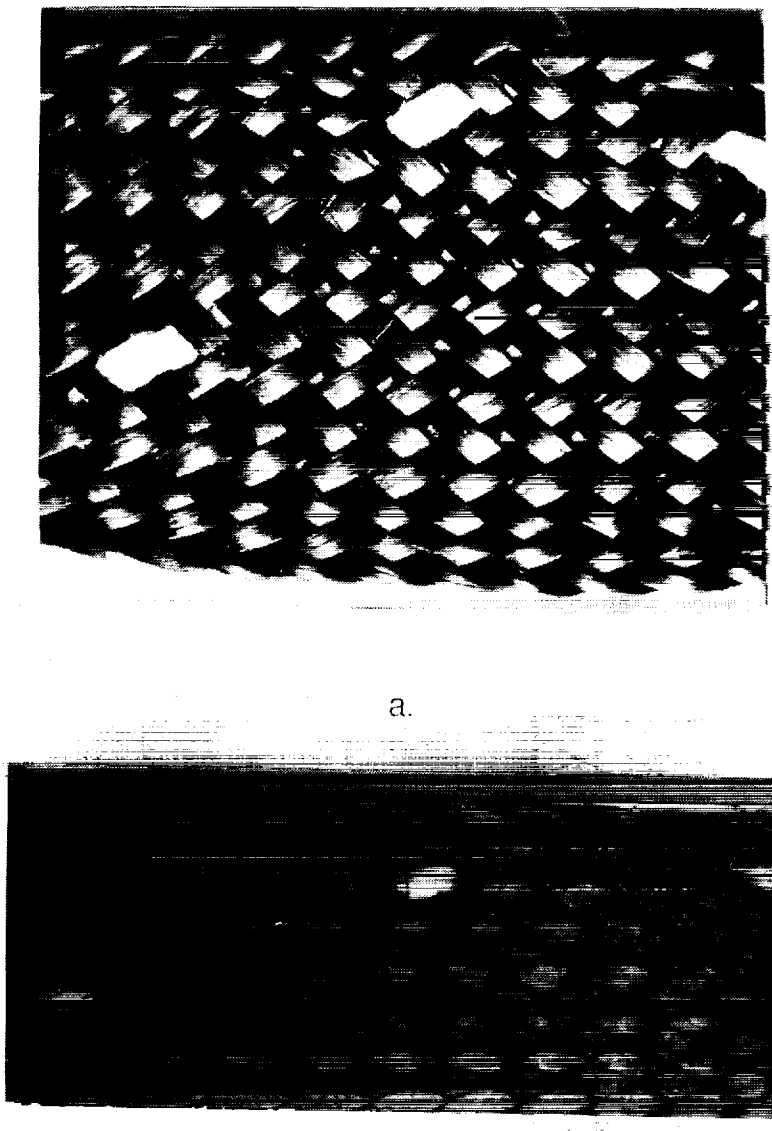

Figure 1 a - Braided Textile Preform; b. - Molded Composite. Note the tracer tow. The composite is 3/4 inch wide.

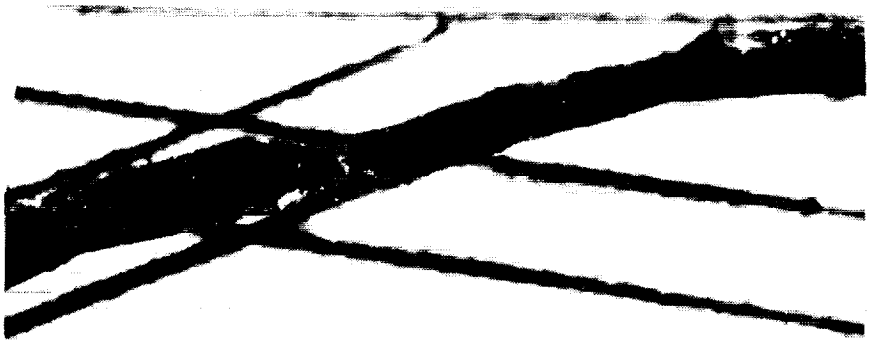

a.

b.

Figure 2. a - Side View of Single Tow. Note the "diamond" where the tow intersects the surface. The lines indicate the apparent braid angle.
b - Top View of Same Tow. Lines indicate the width of the specimen.

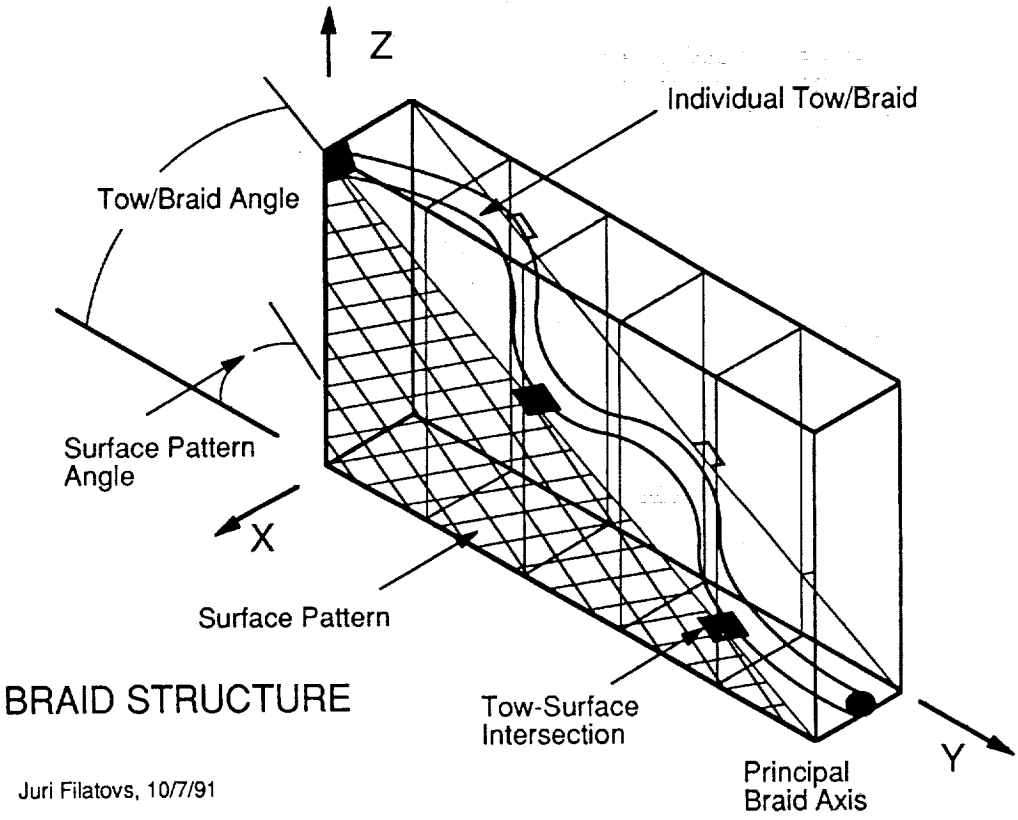

Figure 3. Surface/Volume Mapping of Braid.

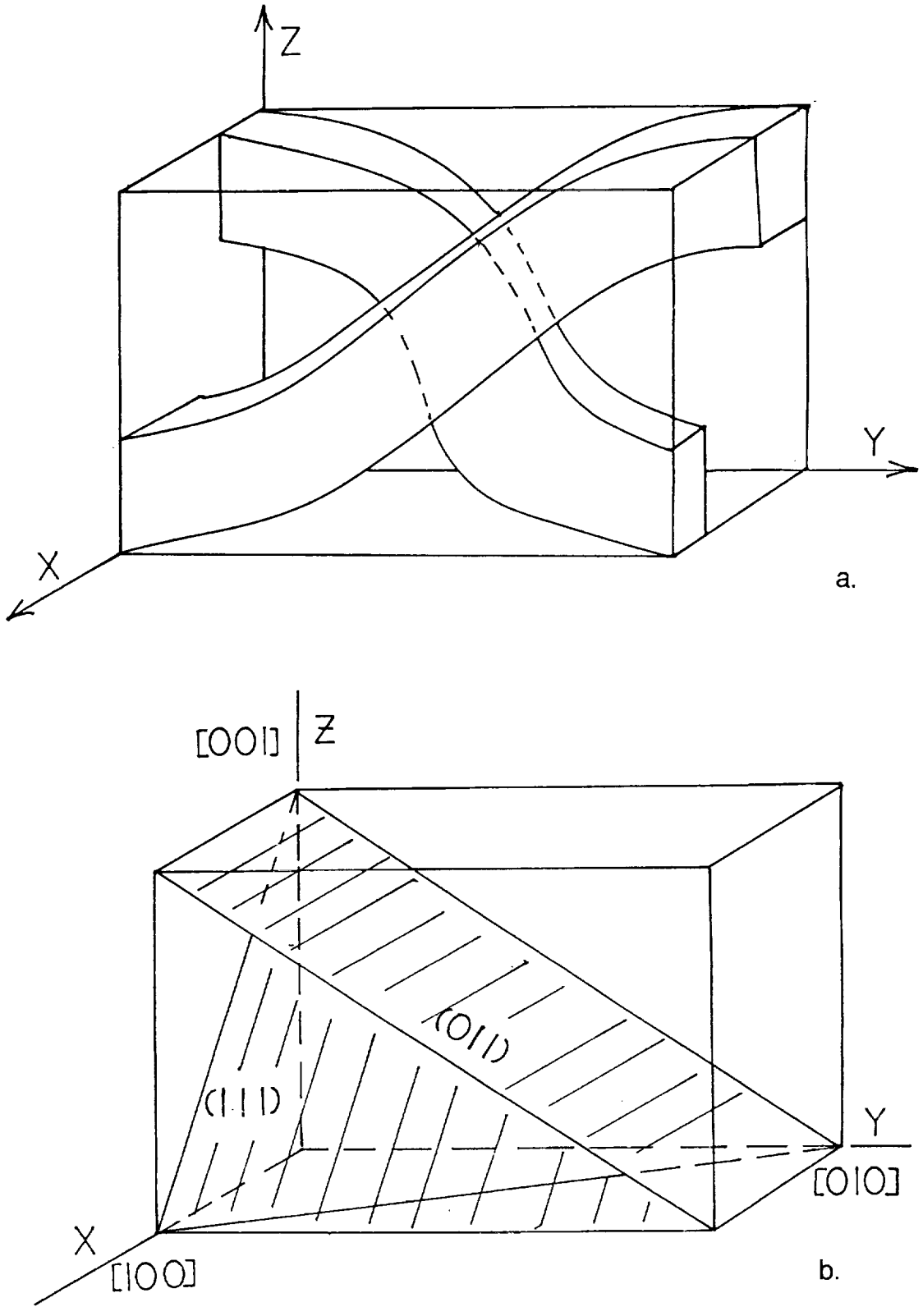

Figure 4. a- Unit Cell. b - Crystallographic Description of Same Pair.

Figure 5. SEM Fractographs of Axial Compression Specimens. Surface is shown.

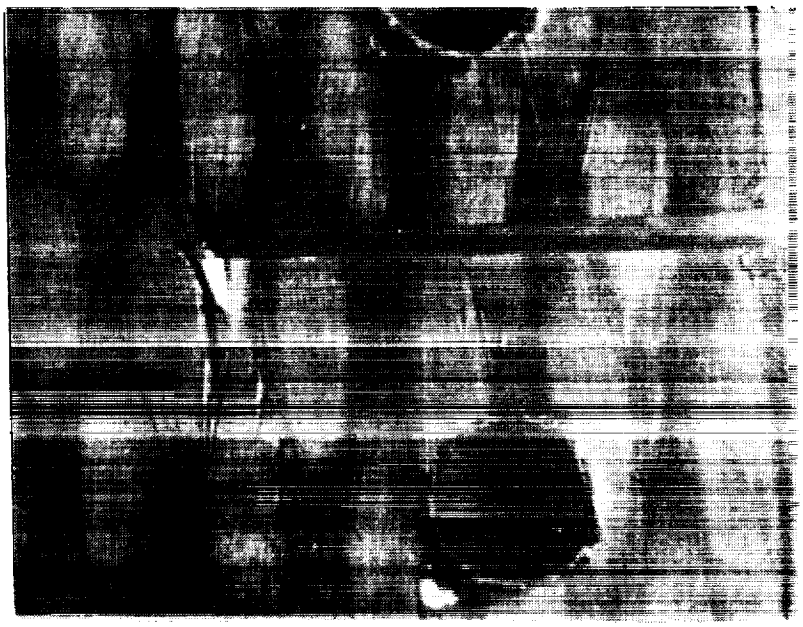

Figure 6. Notched E399-Type Specimen, Notched Perpendicular to Principal Braiding Direction.

Figure 8. "T" Section Failed in 3-Point Bending

Figure 7. Axially Compressed Tube